JOURNAL OF COMPUTATIONAL PHYSICS 14, 371–390 (1974)

Numerical Study of a Cylindrical Plasma Expansion in a Magnetic Field

P. CORNILLE

Commissariat à l'Énergie Atomique, 94190 — Villeneuve Saint-Georges, France

Received January 2, 1973

The cylindrical plasma expansion in a axially symmetric magnetic field is calculated with a magnetohydrodynamic code described herein.

The hydrodynamic and electromagnetic variables are decoupled and computed separately with explicit methods.

A two step Lax–Wendroff method is used for the hydrodynamic equations and a splitting technique applied to the vector potential for the field components.

INTRODUCTION

This paper deals with the numerical computation of a cylindrical plasma expansion in a nonuniform axially symmetric magnetic field so that the plasma variables only depend on r and z directions.

This plasma can be either a laser produced plasma confined by a magnetic field or a plasma trapped in the earth magnetic fields or yet a star in expansion in the vacuum.

A number of analytical solutions of plasma interaction with a magnetic field in one and two dimensions are available throughout the literature.

Some of these works concern spherical and elliptical plasmoids [1–4] other ones cylindrical plasma columns with cylindrical or elliptical cross-sections [5].

None of these works have been able to give a complete solution of the problem including all transport effects. This has naturally led to a numerical approach of the problem. One-dimensional codes have been first developed in spherical and cylindrical coordinates [6–9, 21, 23] and more recently numerical results concerning two-dimensional codes have been published by J. Killeen and J. R. Freeman *et al.* [6, 10, 11].

The study presented here mainly differs from the results of J. Killeen and J. R. Freeman *et al.* by the model chosen and the way by which this problem has been numerically solved. A one fluid magnetohydrodynamic model is used, the calculation being initiated during the laser irradiation of the pellet so that plasma

heating and ionization are taken into account. Charge neutrality and collision-dominance are assumed in this study. All transport effects such as: resistivity, viscosity, and conductibility are included in the calculation.

FORMULATION

The MHD equations are discussed in detail in two books [12, 13]. These equations written in Eulerian conservative form with source terms are

$$\begin{aligned} \frac{\partial \rho}{\partial t} + \nabla \cdot [\rho V] &= \rho_w, \\ \frac{\partial}{\partial t}(\rho V) + \nabla \cdot [K + P - T_M - R] &= 0, \\ \frac{\partial E}{\partial t} + \nabla \cdot \left[\left(\rho e + \frac{1}{2}\rho v^2 + P - R\right) V + S - Q\right] &= E_w, \end{aligned} \tag{1}$$

representing the conservation of mass, momentum and energy. Where ρ, v, e are respectively the density, velocity, and the internal energy per unit mass. In dyadic notation, the remaining quantities are

$$\begin{aligned} E &= \rho e + \frac{1}{2}\rho v^2 + \frac{B^2}{2\mu_0} & K &= \rho VV, \\ P &= pII & Q &= \Gamma\Gamma\nabla T, \\ R &= \frac{\kappa}{2}[\nabla V + (\nabla V)^T] - \frac{\kappa}{3}\nabla VII, & & \\ S &= \frac{1}{\mu_0}(E \wedge B) & T_M &= \frac{1}{\mu_0} BB - \frac{1}{2\mu_0} B^2 II, \end{aligned} \tag{2}$$

$$E + V \wedge B = \eta J + \frac{m_i}{e\rho}[J \wedge B - \nabla p_e],$$

where K, P, R, T stand for the kinetic, pressure, viscous, and magnetic stress tensors. While Q, S, V are respectively the heat flux, electromagnetic energy, and velocity vectors, with $\Gamma\Gamma$ as the tensor of conductibility and κ the coefficient of shear viscosity. For an isotropic monoatomic, ideal gas, we have the relations

$$\rho = mN \qquad p = NkT \qquad \rho e = \frac{p}{\gamma - 1} \qquad \gamma = \frac{5}{3}. \tag{3}$$

The field components are calculated from the θ component of the vector potential rather from the generalized Ohm's law. In this study the term $[J_\wedge B - \nabla P_e]$ has

no θ component so that the θ component of the vector potential in the plasma is given by the simple equation:

$$\frac{\partial A}{\partial t} = \frac{\eta}{\mu_0} \Delta A + V_\wedge(\nabla_\wedge A).$$

In the vacuum we have to solve a Laplace like equation:

$$\Delta A = \frac{\partial}{\partial r} \frac{1}{r} \frac{\partial}{\partial r} rA + \frac{\partial^2 A}{\partial z^2} = 0. \tag{4}$$

At the plasma-vacuum interface we did use the boundary condition: $[E] = 0$ where the brackets mean a jump of the quantity through the interface. The field components are then obtained everywhere on the mesh by the relations

$$B = \nabla_\wedge A \qquad \text{and} \qquad E = -\frac{\partial A}{\partial t}. \tag{5}$$

Numerical Scheme

The hydrodynamic equations (1) written in a conservative form can be represented in a symbolic form

$$\frac{\partial U}{\partial t} + \nabla \cdot F(U) = W, \tag{6}$$

where W is the source term.

For cylindrical coordinates with axial symmetry, this equation can be written in the different forms depending on r:

$$\begin{aligned} &\frac{\partial U}{\partial t} + \frac{2\partial F}{\partial r}(U) + \frac{\partial}{\partial r} G(U) + \frac{\partial}{\partial z} H(U) = W \qquad r = 0, \\ &\frac{\partial U}{\partial t} + \frac{1}{r} \frac{\partial}{\partial r} rF(U) + \frac{\partial}{\partial r} G(U) + \frac{\partial}{\partial z} H(U) = W \qquad r \geqslant \Delta r, \end{aligned} \tag{7}$$

where $F(U)$, $G(U)$, and $H(U)$ stand for the r- and z-components of the developed equations described in (1).

For such a system, we use the well known two-step Lax-Wendroff method [14, p. 361] which is given by the finite difference scheme

$$\begin{aligned} U_{l,m}^{n+1} = {} & \frac{1}{4}[U_{l+1,m}^n + U_{l-1,m}^n + U_{l,m+1}^n + U_{l,m-1}^n] - \frac{\Delta t}{2\Delta r} \frac{1}{r_l} [r_{l+1} F_{l+1,m}^n - r_{l-1} F_{l-1,m}^n] \\ & - \frac{\Delta t}{2\Delta r} [G_{l+1,m}^n - G_{l-1,m}^n] - \frac{\Delta t}{2\Delta z} [H_{l,m+1}^n - H_{l,m-1}^n] \\ & + \frac{\Delta t}{4} [W_{l+1,m}^n + W_{l-1,m}^n + W_{l,m+1}^n + W_{l,m-1}^n], \end{aligned} \tag{8}$$

$$U_{l,m}^{n+2} = U_{l,m}^{n} - \frac{\Delta t}{\Delta r}\,[r_{l+1}F_{l+1,m}^{n+1} - r_{l-1}F_{l-1,m}^{n+1}]/r_l$$

$$- \frac{\Delta t}{\Delta r}\,[G_{l+1,m}^{n+1} - G_{l-1,m}^{n+1}] - \frac{\Delta t}{\Delta z}\,[H_{l,m+1}^{n+1} - H_{l,m-1}^{n+1}] + 2\,\Delta t\, W_{l,m}^{n}\,. \quad (9)$$

This explicit scheme involves the calculation of U, F, G, H, W on a nine-point molecule as shown in Fig. 1.

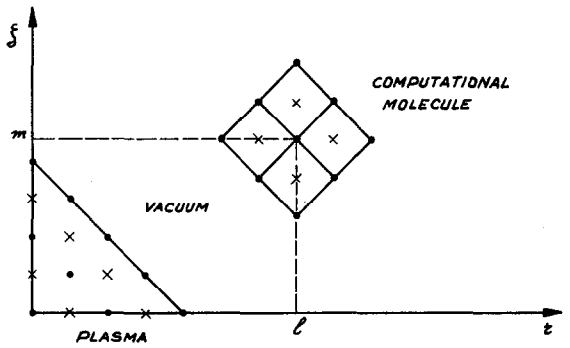

FIG. 1. Computational molecule and plasma configuration at time zero.

Provisional values on the four cross-points are first calculated at time $n + 1$ with Eq. (8) and the final value at time $n + 2$ are then obtained from Eq. (9).

The stability condition for a two-cartesian coordinate scheme was given by Richtmeyer and K. W. Morton [14] and was used as an indication in this study

$$(V + C)\frac{\Delta t}{\Delta r} < \frac{1}{\sqrt{2}} \qquad \text{with} \quad \Delta r = \Delta z, \quad (10)$$

where V and C are the fluid and magnetosonic velocities given by

$$V = (V_r^2 + V_z^2)^{1/2} \qquad \text{and} \qquad C = (C_S^2 + C_A^2)^{1/2}, \quad (11)$$

with C_S and C_A as the sound and Alfven speeds given by the relations

$$C_S = \left(\frac{\gamma kT}{m}\right)^{1/2} \qquad \text{and} \qquad C_A = \left(\frac{B_r^2 + B_z^2}{\mu_0 mN}\right)^{1/2}. \quad (12)$$

The stability condition (10) is calculated and should be verified everywhere in the plasma. As shown by Eq. (12), low densities can lead to high Alfven speeds and therefore to a small and indesirable timestep for insuring stability. So a minimum density $N_{\min}$ is chosen as small as possible in order to give an acceptable timestep.

During the calculation the density N is compared to $N_{\min}$, if $N \geqslant N_{\min}$ we are in the plasma, otherwise we are in the vacuum. This test defines the boundary of the plasma-vacuum interface which is arbitrary located on the last point calculated. Then all hydrodynamic variables are set equal to zero in the vacuum. There is another approach [6] which consists to suppose the presence of a background plasma throughout the mesh, this approach is less physical and by so doing we create a shock at the boundary. In this case the variables calculated by the Eqs. (1) are no longer conserved.

From a mathematical point of view we suppose that the components: $F(U)$, $G(U)$, and $H(U)$ of Eq. (7) vary continuously across the plasma-vacuum interface: the hydrodynamic variables decreasing and the field components increasing across the boundary so that the result of these two compensating effects is smooth and continuous enough to allow the use of the numerical scheme (8) and (9) at the interface.

As suggested by Potter *et al.* [15, pp. 399 and 16] the viscosity and conductibility terms are introduced at the second step of the scheme.

The tensor of conductibility $\Gamma\Gamma$ and the coefficient of schear viscosity κ are calculated at time $n+1$ on the four cross points (Fig. 1) and the derivatives are then computed at time n with finite differences centered on the cross points. The introduction of diffusion terms in the schemes (8) and (9) can make the equations more parabolic than hyperbolic depending on the value of the coefficients of diffusion, leading to a more severe stability condition than condition (10). The stability condition for a parabolic equation will be studied later for the calculus of the vector potential.

The fiels components: Br, Bz, $E\theta$ are obtained from the component $A_{l,m}$ of the vector potential as follows:

$$
\begin{aligned}
B_{r_{l,m}}^{n+1} &= -\frac{1}{2\,\Delta r}\,[A_{l,m+1}^{n+1} - A_{l,m-1}^{n+1}], \\
B_{z_{l,m}}^{n+1} &= \frac{1}{r_l 2\,\Delta r}\,[r_{l+1}A_{l+1,m}^{n+1} - r_{l-1}A_{l-1,m}^{n+1}], \\
E_{\theta_{l,m}}^{n+1} &= -\frac{1}{\Delta t}\,[A_{l,m}^{n+1} - A_{l,m}^{n}].
\end{aligned}
\tag{13}
$$

The field components are thus computed everywhere on the mesh.

In the plasma, the vector potential A has to be calculated from the parabolic equation

$$
\frac{\partial A}{\partial t} = \frac{\eta}{\mu_0}\left[\frac{\partial}{\partial r}\frac{1}{r}\frac{\partial}{\partial r}rA + \frac{\partial^2 A}{\partial z^2}\right] - V_r\frac{1}{r}\frac{\partial}{\partial r}rA - V_z\frac{\partial A}{\partial z}. \tag{14}
$$

We make use of a splitting technique (17) which is second order accurate where each term is treated by the Lax–Wendroff method. We have

$$A_{l,m}^{n+1} = \left[1 + \Delta t\, \mathscr{L} + \frac{\Delta^2 t}{2}\, \mathscr{L}^2\right] A_{l,m}^{n} \tag{15}$$

We split the operator $\mathscr{L}$ into two operators $\mathscr{L}_r$ and $\mathscr{L}_z$ such that

$$\tilde{A}_{l,m} = \left[1 + \Delta t\, \mathscr{L}_r + \frac{\Delta^2 t}{2}\, \mathscr{L}_r^2\right] A_{l,m}^{n}, \tag{16}$$

$$A_{l,m}^{n+1} = \left[1 + \Delta t\, \mathscr{L}_z + \frac{\Delta^2 t}{2}\, \mathscr{L}_z^2\right] \tilde{A}_{l,m}, \tag{17}$$

with the finite difference operators defined by

$$\begin{aligned} &\mathscr{L}_r = a\,\delta^2 - b\,\delta\mu - c \qquad \mathscr{L}_r^2 = (b^2 - 2ac)\,\delta^2 + 2bc\,\delta\mu + c^2, \\ &\mathscr{L}_z = a\,\delta^2 - d\,\delta\mu \qquad\quad \mathscr{L}_z^2 = d^2\,\delta^2, \\ &a = \eta/\mu_0 \qquad b = V_r - a/r \qquad c = \frac{V_r}{r} + \frac{a}{r^2} \qquad d = V_z, \end{aligned} \tag{18}$$

where δ and $\delta\mu$ stand for the finite difference operators

$$\begin{aligned} \delta_x A(x) &= [A(x + 1/2) - A(x - 1/2)]/\Delta x, \\ \delta_x \mu_x A(x) &= [A(x + 1) - A(x - 1)]/2\,\Delta x. \end{aligned} \tag{19}$$

The stability of this scheme is obtained by insuring the stability of each equation (16) and (17). A Fourier analysis of the parabolic equation

$$\frac{\partial A}{\partial t} = a\,\frac{\partial^2 A}{\partial x^2} - b\,\frac{\partial A}{\partial x} - cA \tag{20}$$

gives the following amplification factor β

$$|\beta(\alpha)|^2 = (1 - 2C + A\cos\alpha)^2 + 4B^2 \sin^2\alpha \leqslant 1,$$

with

$$\begin{aligned} A &= \left[\frac{a}{\Delta x} + \frac{\Delta t}{\Delta x}\left(\frac{b^2}{2} - ac\right)\right]\frac{\Delta t}{\Delta x}, \\ B &= \frac{b}{2}(1 - \Delta t\, c)\,\frac{\Delta t}{\Delta x}, \\ C &= A + c\,\frac{\Delta x}{2}\left(1 - \Delta t\,\frac{c}{2}\right)\frac{\Delta t}{\Delta x}. \end{aligned} \tag{21}$$

For insuring stability, the following conditions should be satisfied:

$$0 \leqslant C + A \leqslant 1 \qquad \text{and} \quad 0 \leqslant C - A \leqslant 1 \tag{22}$$

and either

$$4A^2 \leqslant 4B^2 \leqslant \frac{4A^2}{C + A} \qquad \text{or} \qquad |2B| \leqslant |2A|,$$

when $c = 0$ for the z-direction, we have the more simple conditions

$$4B^2 \leqslant |2A| \leqslant |2B| \leqslant 1 \qquad \text{or} \quad |2B| \leqslant |2A| \leqslant 1.$$

Since the coefficients a, b, c are nonconstant, these stability conditions are local. These coefficients are calculated at each timestep n on the points and interpolated on the crosses (Fig. 1).

We can now calculate the vector potential A in the vacuum at times $n + 1$ and $n + 2$ by solving the Laplace's equation

$$\frac{\partial}{\partial r}\frac{1}{r}\frac{\partial}{\partial r} rA + \frac{\partial^2}{\partial z^2} A = 0. \tag{23}$$

We use an iterative method, the successive over relaxation method of Tchevycheff (SORT) described by Hockney [15, p. 167] which has been extended to cylindrical coordinates. This method defines new values A^{p+1} from old ones A^p with the iterative equation

$$A_{l,m}^{p+1} = \frac{\omega^{p+1}}{\alpha}\left[A_{l,m-1}^{p+1} + (1 - \beta) A_{l-1,m}^{p+1} + (1 + \beta) A_{l+1,m}^{p} + A_{l,m+1}^{p}\right] + (1 - \omega^{p+1}) A_{l,m}^{p} \tag{24}$$

with

$$\alpha = 4(1 + \beta^2) \qquad \text{and} \quad \beta = 1/2(l - 1).$$

The SORT process consists of sweeping a $N \times P$ mesh with this equation point by point on points for which $l + m$ is odd during one iteration and then on all $l + m$ even points during the next one.

Where the over relaxation parameter ω^{p+1} is changed every iteration according to the following scheme:

$$\omega^0 = 1 \quad \omega^1 = 1/(1 - \tfrac{1}{2}\mu^2) \quad \omega^{p+1} = 1/(1 - \tfrac{1}{4}\mu^2\omega^p) \qquad \text{for} \quad p \geqslant 1, \tag{25}$$

with

$$\mu = 1 - \tfrac{1}{4}((\gamma^2/N^2) + (\pi^2/P^2)) \qquad \text{and} \quad \gamma = 3.831, \qquad \pi = 3.141.$$

This operation is repeated for $p = 0, 1, 2,...$, until convergence has been obtained. This is practically done for 20 iterations. The old values of A ($p = 0$) are used to start the iteration.

We should define the position of the boundary and the values of A on it in order to solve this iterative scheme. We know that the boundary is located between two successive points of the numerical scheme (8) (9) separated by an interval $2\Delta r$ or $2\Delta z$, moreover the field components in the last points calculated in the plasma region are obtained by the relations (13) and computed with mean odd central differences so that the points $(l, m + 1)$ and $(l + 1, m)$ should belong to the plasma-vacuum interface and serve as boundary conditions for the vacuum equation (4).

After calculation of the vector potential in the plasma, the values of A on the boundary are computed from the relations:

$$E^v_{l+1,m} = E^P_{l,m} \qquad \text{or} \qquad E^v_{l,m+1} = E^P_{l,m}\,, \tag{26}$$

where v and p respectively mean: vacuum and plasma. These relations imply the continuity of E_θ through the boundary.

Numerical Model

The initial values of the MHD variables must be specified everywhere on the mesh in order to begin the calculation. In the plasma, the hydrodynamic variables are

$$N_{l,m} = N_0 \exp - a[(l-1)^2 + (m-1)^2]^{1/2},$$
$$V^r_{l,m} = V_0(l-1) \qquad V^z_{l,m} = V_1(m-1) \qquad T_{l,m} = T_0\,. \tag{27}$$

The particle and energy source terms are

$$E^w_{l,m} = E_w W^n D_E(l, m) \qquad N^w_{l,m} = N_w W^n D_N(l, m). \tag{28}$$

The terms W^n and $D(l, m)$ stand for the time source term and the Dirac's function.

The source term for a Gauss shape pulse laser is given by the relation

$$W^n = \left[1 + \operatorname{erf}\frac{t - t_0}{\Delta t_0\sqrt{2}}\right]\Big/2 \qquad \text{with} \quad t = n\,\Delta t. \tag{29}$$

The Dirac's function is defined by the simple relation

$$D(l, m) = 1/MV^l. \tag{30}$$

Where M and V^l are respectively the number of points taken into account for calculated $D(l, m)$ and the volume of each mesh cell centered on l.

The program has been designed to use any analytical source terms one can provide. However these source terms have been chosen on a mathematical ground rather than on a physical ground in order to check the two step Lax–Wendroff method (8) and (9) with source terms.

The energy and the number of particle computed with the numerical scheme (8) and (9) are first summed on the mesh and then on the time, and finally plotted on graphs (8) and (10). In this case it is an easy matter to check the results with the theoretical energy and particle number given by the integral relations

$$\begin{aligned} E^{n\Delta t} &= E_0 + E_w \int_0^{n\Delta t} \left[1 + \operatorname{erf} \frac{(t - t_0)}{\Delta t_0 \sqrt{2}}\right] \Big/ 2 \, dt, \\ N^{n\Delta t} &= N_0 + N_w \int_0^{n\Delta t} \left[1 + \operatorname{erf} \frac{(t - t_0)}{\Delta t_0 \sqrt{2}}\right] \Big/ 2 \, dt. \end{aligned} \tag{31}$$

A mirror magnetic field is used and is defined by the relations

$$\begin{aligned} B_r &= -\alpha A_0 I_1(\beta r) \sin(\beta z), \\ B_z &= A_0[1 - \alpha I_0(\beta r) \cos(\beta z)], \\ A_\theta &= A_0[r/2 - I_1(\beta r) \cos(\beta z)]. \end{aligned} \tag{32}$$

Where I_0 and I_1 are modified Bessel functions of the first kind and α, β, A_0 are given constants.

The transport coefficients are given by Spitzer [18] and can be written in the form:

$$\begin{aligned} \eta &= \eta_0 T^{-3/2} && \text{resistivity,} \\ \gamma_\perp &= \gamma_0 T^{5/2} && \text{transverse conductibility,} \\ \gamma_\parallel &= \gamma_1 T^{5/2} && \text{parallel conductibility,} \\ \kappa &= \kappa_0 T^{5/2} && \text{shear viscosity.} \end{aligned} \tag{33}$$

For insuring a proper conservation of the quantities $U_{l,m}^{n+2}$ calculated with the conservative scheme (8) and (9) we have to set to zero the flux of the variables $U_{l,m}^{n+1}$ in one or all the components $F_{l+1,m}^{n+1}$, $H_{l,m+1}^{n+1}$, $H_{l,m-1}^{n+1}$ at the plasma-vacuum interface depending on the form of the boundary.

The conservative property of this scheme has been checked on the mass, including smoothing, without source terms. The difference obtained was: $\Delta m \simeq 5.7\ 10^3$ after 200 timesteps ($\Delta t = 15$ps) for an initial mass $m = 4.09\ 10^{15}$.

A 50×50 square mesh has been chosen with plasma filling the 5-point left corner as shown on Fig. 1, for starting the computation.

As pointed out by Richtmyer [14, p. 366] instabilities show up in regions of rapid change of the flow.

In this model, these instabilities occur near the center of the plasma. So a smoothing technique reported by Lapidus [19] has been used in this study. This technique can be seen as the fractional step of the diffusion equation

$$\frac{\partial U}{\partial t} = \lambda \frac{1}{r} \frac{\partial}{\partial r} r \left[\frac{\partial \mid V_r \mid}{\partial r} \frac{\partial U}{\partial r} \right] + \lambda \frac{\partial}{\partial z} \left[\frac{\partial \mid V_z \mid}{\partial z} \frac{\partial U}{\partial z} \right] \tag{34}$$

This parabolic equation can be then written in the numerical form:

$$\begin{aligned} \tilde{U}_{l,m} &= U_{l,m}^{n+2} + \lambda \frac{\Delta t}{\Delta^3 r} \frac{1}{r_l} \delta_r r_l [\delta_r \mid V_{l,m}^r \mid \delta_r U_{l,m}^{n+2}], \\ U_{l,m}^{n+3} &= \tilde{U}_{l,m} + \lambda \frac{\Delta t}{\Delta^3 z} \delta_z [\delta_z \mid V_{l,m}^z \mid \delta_z \tilde{U}_{l,m}]. \end{aligned} \tag{35}$$

Where the operators δ_r, δ_z stand for now for the mean odd central differences defined as follows:

$$\delta_x f(x) = [f(x + h) - f(x - h)]/2.$$

Variables	Value	Units
N_0	10^{21}	nb/cm^3
N_w	$5\ 10^{24}$	nb/cm^3
$N_{\min}$	$8\ 10^{16}$	nb/cm^3
V_0	$1.5\ 10^{6}$	cm/s
V_1	$1.5\ 10^{6}$	cm/s
T_0	$2\ 10^{5}$	°K
E_w	$5\ 10^{16}$	erg/s
t_0	15	ns
Δt_0	7.5	ns
Δt	$7.5\ 10^{-3}$	ns
A_0	$2\ 10^{5}$	gauss
Δr	10^{-2}	cm
η_0	$3\ 10^{14}$	cgs
γ_0	10^{-8}	cgs
γ_1	10^{-8}	cgs
κ_0	$3\ 10^{-17}$	cgs
λ	$8\ 10^{-4}$	cgs

FIG. 2. Initial values and data in C.G.S. units

The smoothing technique of Lapidus consists to take the values $U_{l,m}^{n+3}$ as the final values at time $n + 2$.

All the data used to initiate the calculation are displayed on Fig. 2 with C.G.S. units. They have mainly been taken from the reports [9, 21–23]. The calculus has been stopped after 1500 steps with a 7.5 ps timestep.

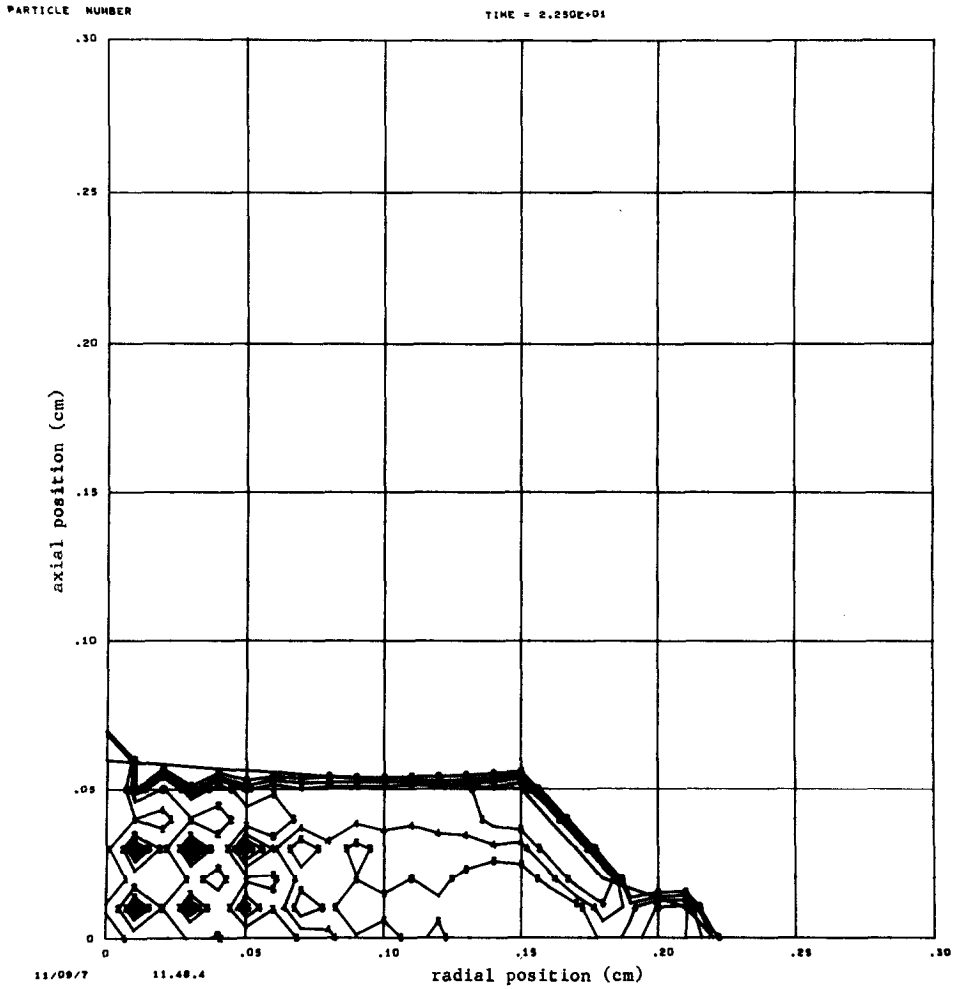

FIG. 3. Profile of particle number in the plasma at time 22.5 nsec.

RESULTS

It is quite difficult to display all the output values of this code, so we only show the set of figures concerning the output values obtained at the last timestep.

Figures 3, 4, and 5 represent respectively the profiles of particle number, temperature and electric field, then Figs. 6 and 7 show the velocity and magnetic fields. In Figs 8 and 9 we have the particle number and the kinetic energy of the plasma

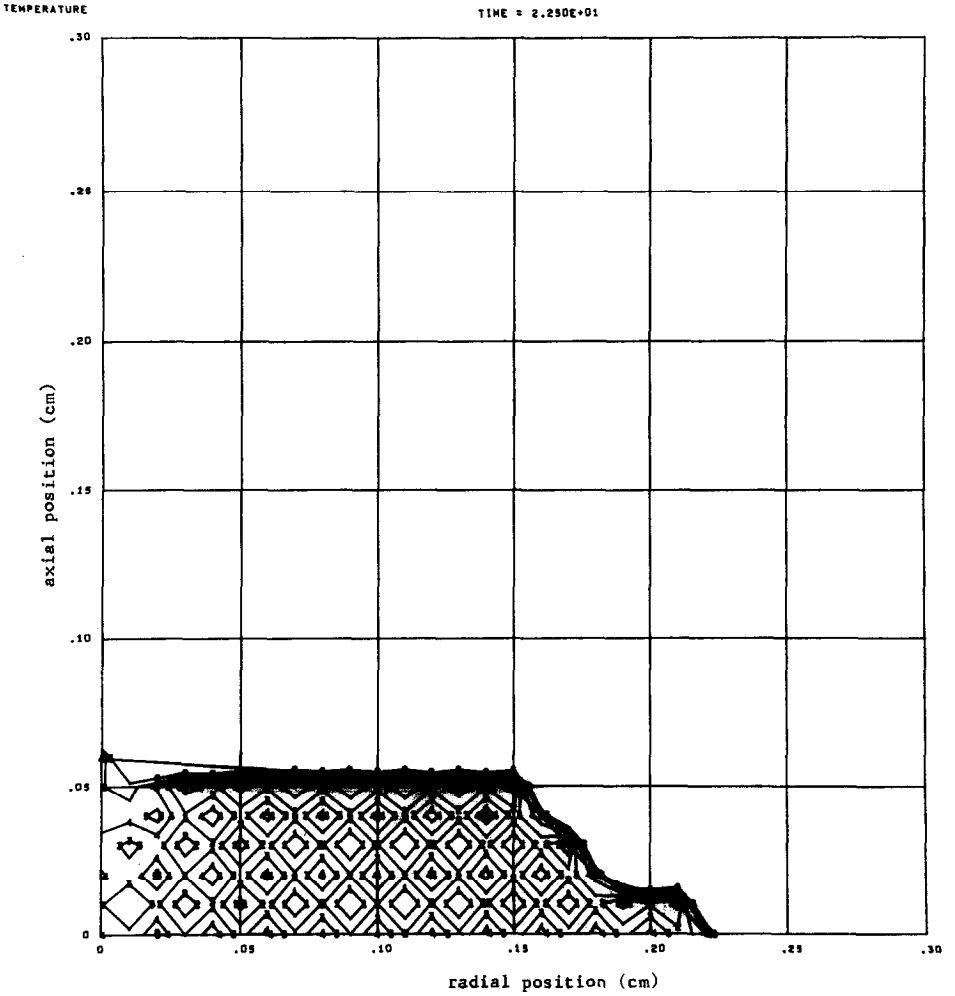

FIG. 4. Profile of temperature in the plasma at time 22.5 nsec.

versus time, the last figure show by order of magnitude: the energy created by the laser and totally absorbed in the plasma, the thermal and kinetic energies of the plasma versus time.

If we look at Fig. 3, we see that the plasma has expanded approximately four times farther in the radial direction than the axial direction, this is rather surprising from a physical point of view. One can explain this fact by noticing that the Dirac's source term does not depend on the z direction. Consequently, this source term

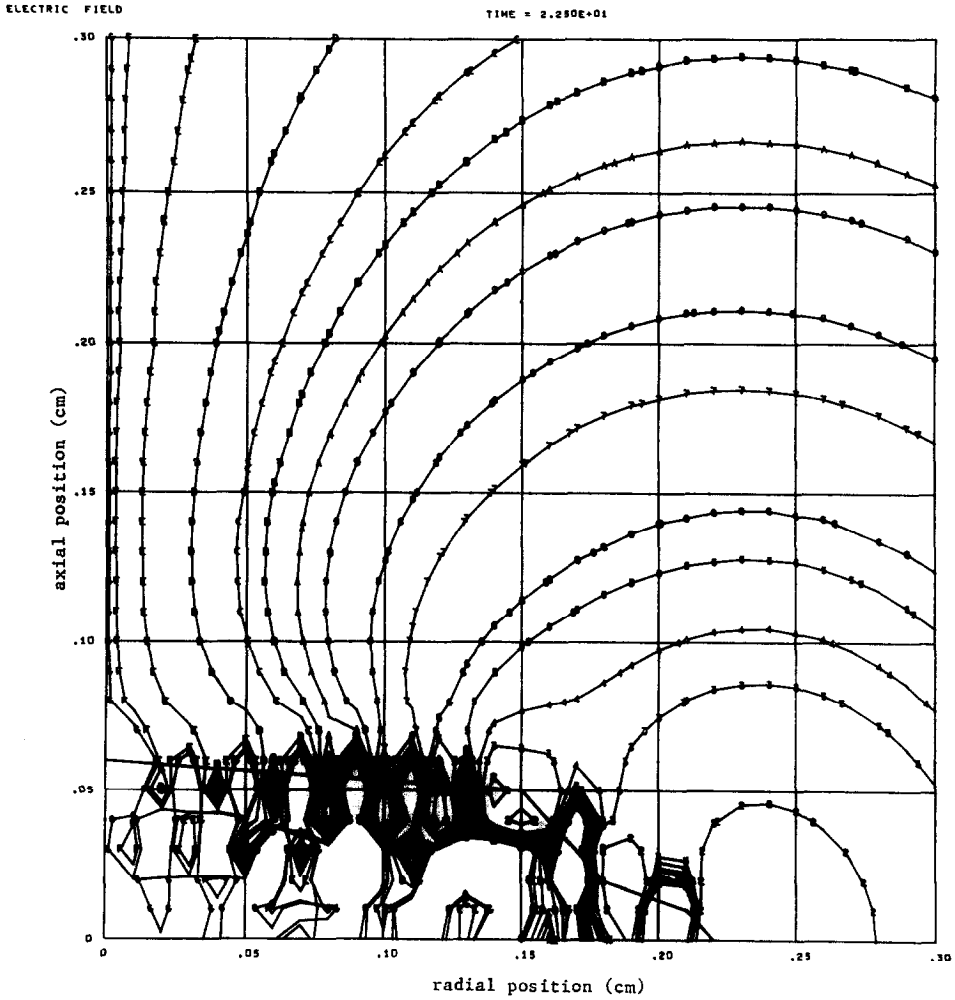

FIG. 5. Profile of the electric field E_0 throughout the mesh.

imposes a strong gradient in the radial direction only so that we have mainly a cylindrical expansion of the plasma. However this expansion decelerates at about 12 nsec and even decreases until the time 20 nsec for increasing again as shown on Fig. 9.

The other features which are puzzling are the regular pattern of Fig. 7 and the oscillations in the velocity and magnetic fields in the plasma (Figs. 6 and 7).

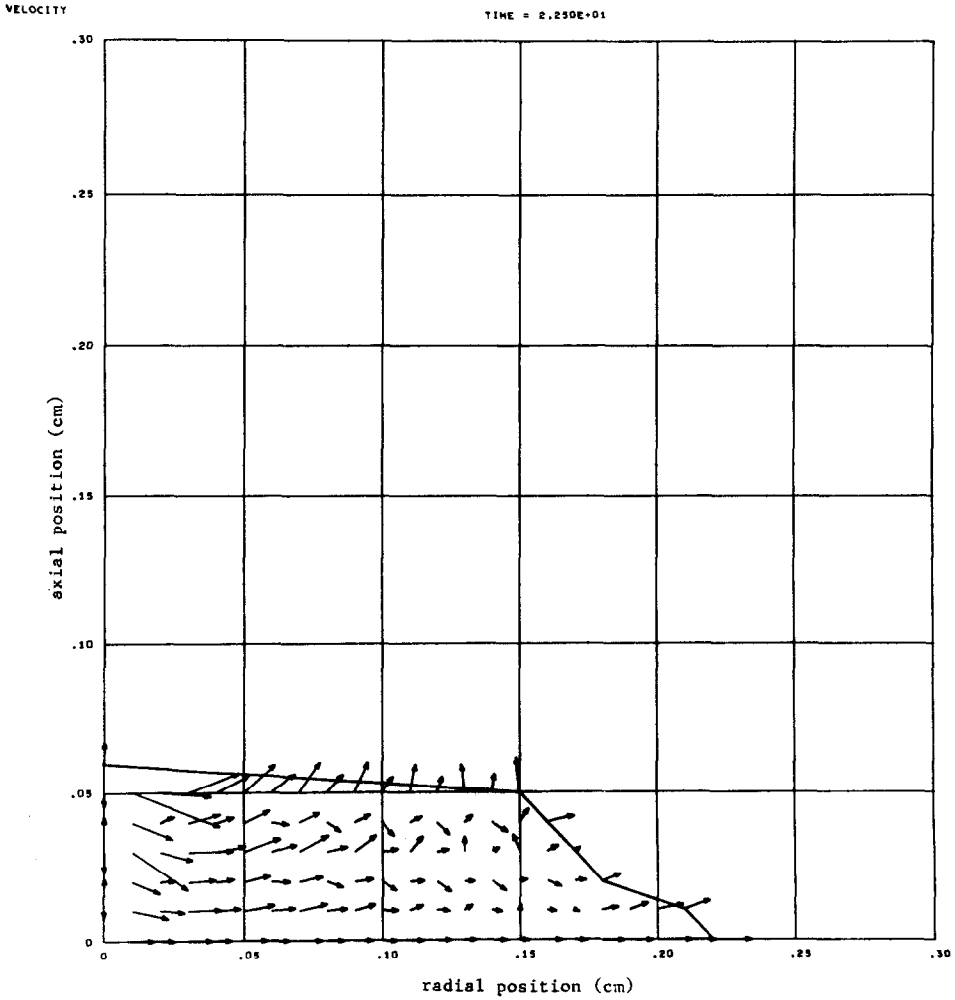

FIG. 6. Velocity field in the plasma at time 22.5 nsec.

This is due to the fact that the numerical scheme ((8) and (9)) has two uncoupled meshes (see for example Roberts and Potter [15, p. 377]).

Since the resistivity decreases with temperature the magnetic field is more and more related to the velocity field as the computation proceeds and should therefore present the same oscillations. In the same manner the conductibility increasing with the temperature, the values of the temperature of each independent mesh are

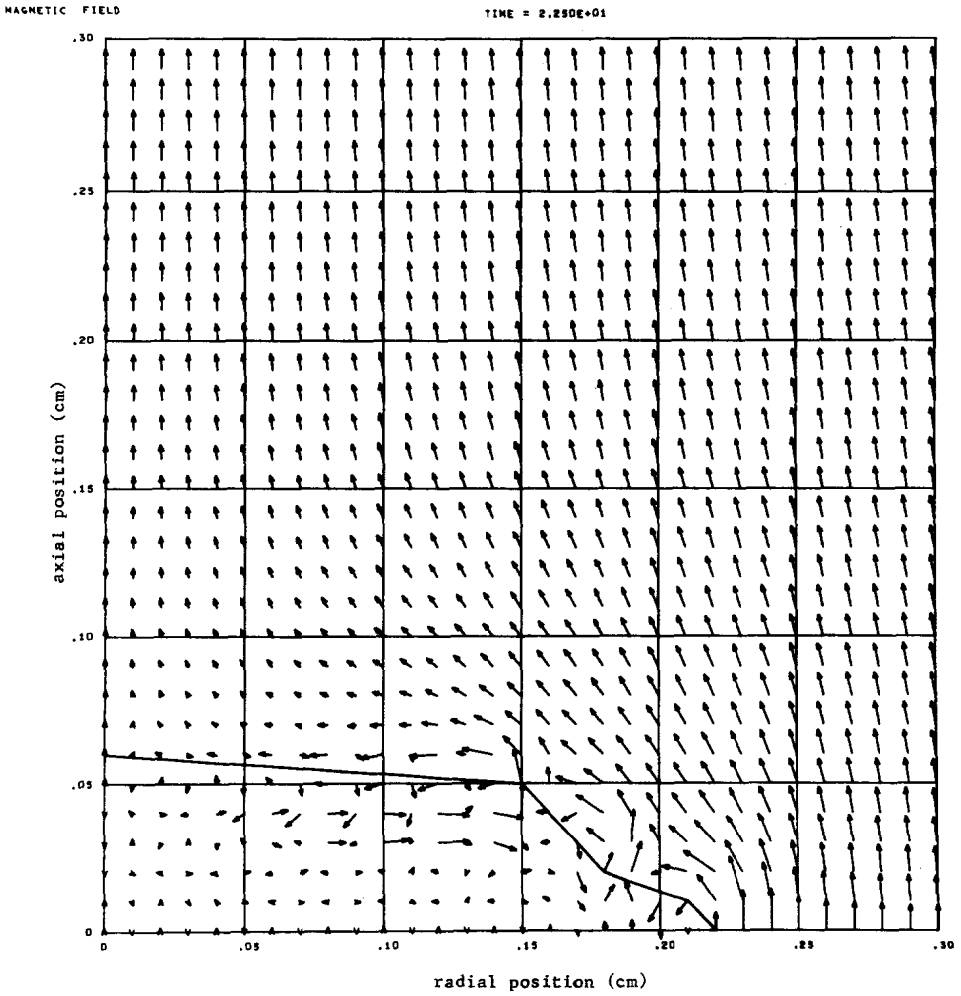

FIG. 7. Magnetic field throughout the mesh.

strongly coupled together at the end of the calculation giving the regular pattern shown on Fig. 4.

This undesirable feature is a common problem to all numerical schemes with independant meshes, this problem has been also studied in a paper to be presented by Hirt and Amsden [20]). So these two independant meshes should be linked together if we want to avoid the apparition of two velocity fields. This can be done

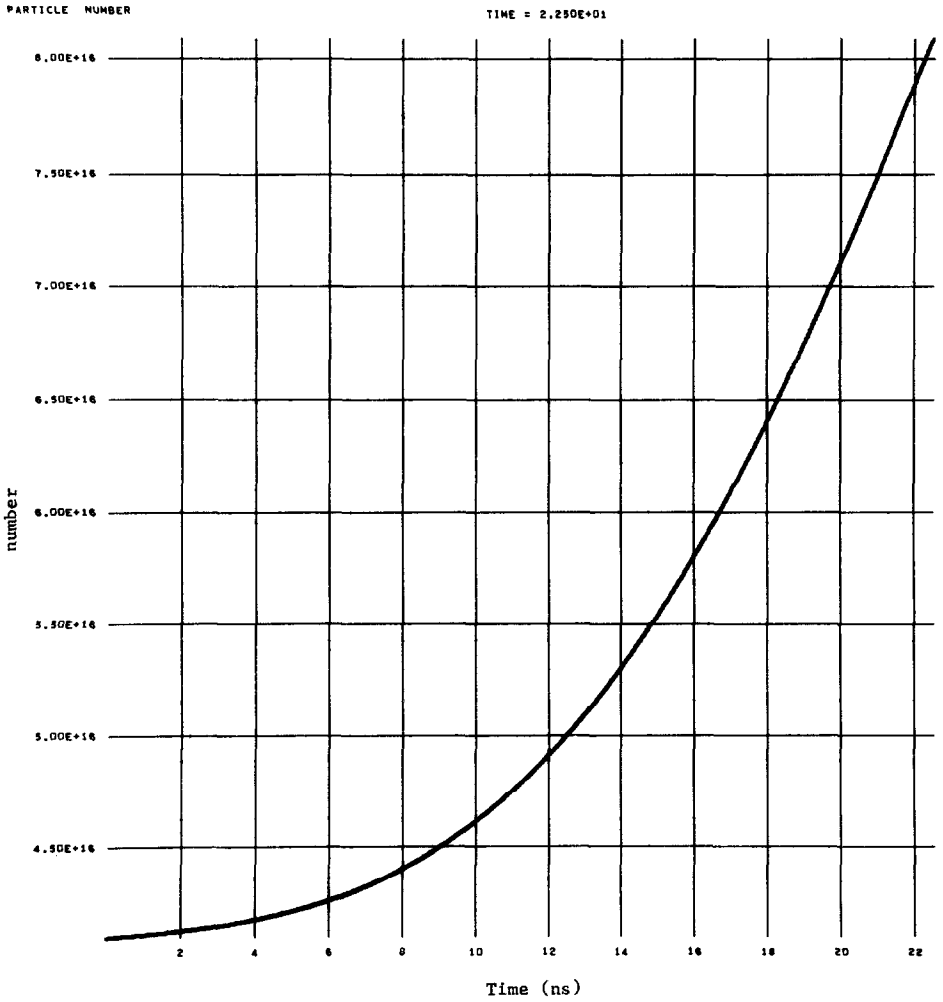

FIG. 8. Particle number in the plasma versus the time.

by the viscosity since the terms introduced at the second step (9) coupled the two meshes.

Unfortunely the physical value of the viscosity is too small for having any effect on the numerical values and the oscillations have the time to build up progressively through the computation before the temperature is high enough to begin to couple the two meshes. So we choose a value of the constant $\kappa_0 = 3.10^{-17}$

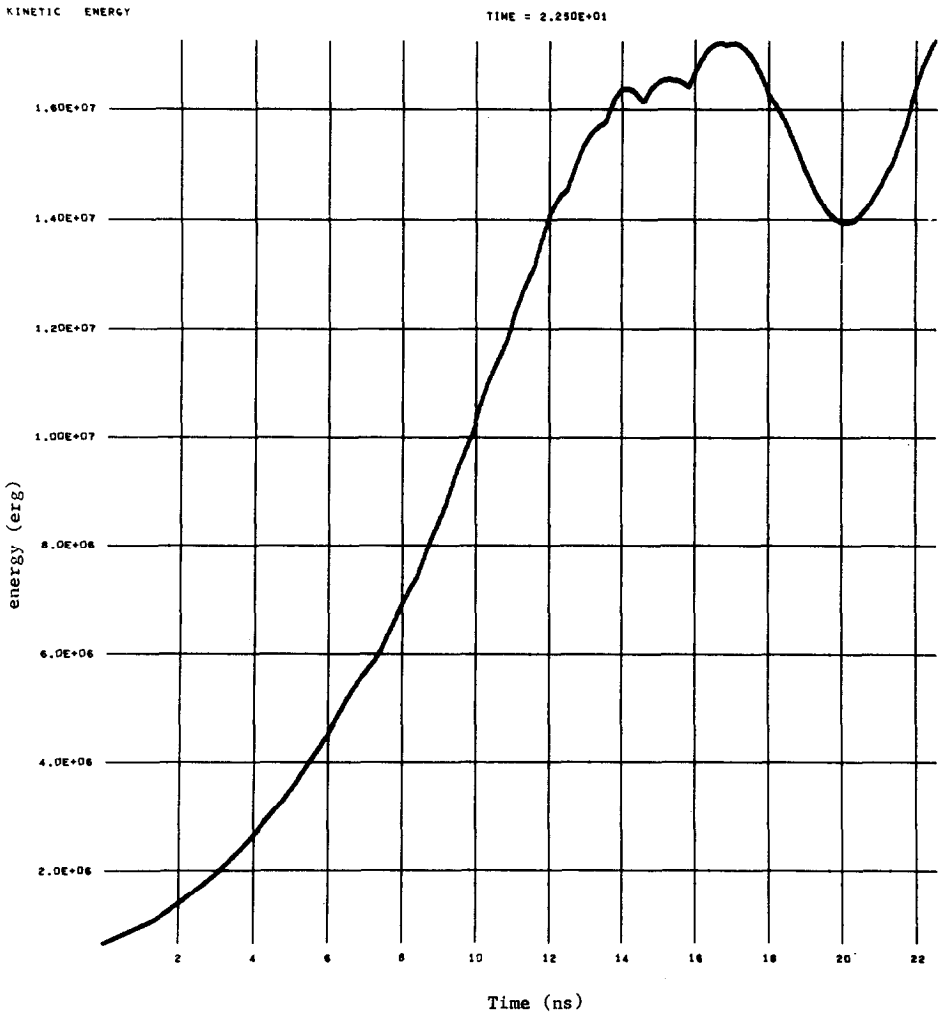

FIG. 9. Kinetic energy in the plasma versus the time.

about 20 times greater than the physical value with a sensible improvement in the results. However the final results presented here show that the value of the viscosity is not great enough to couple efficiently these two meshes.

One can still increase the value of the viscosity or use another approach suggested by Hirt and Amsden [20] which can be applied at each time step or periodically in order to remove the undesirable oscillations.

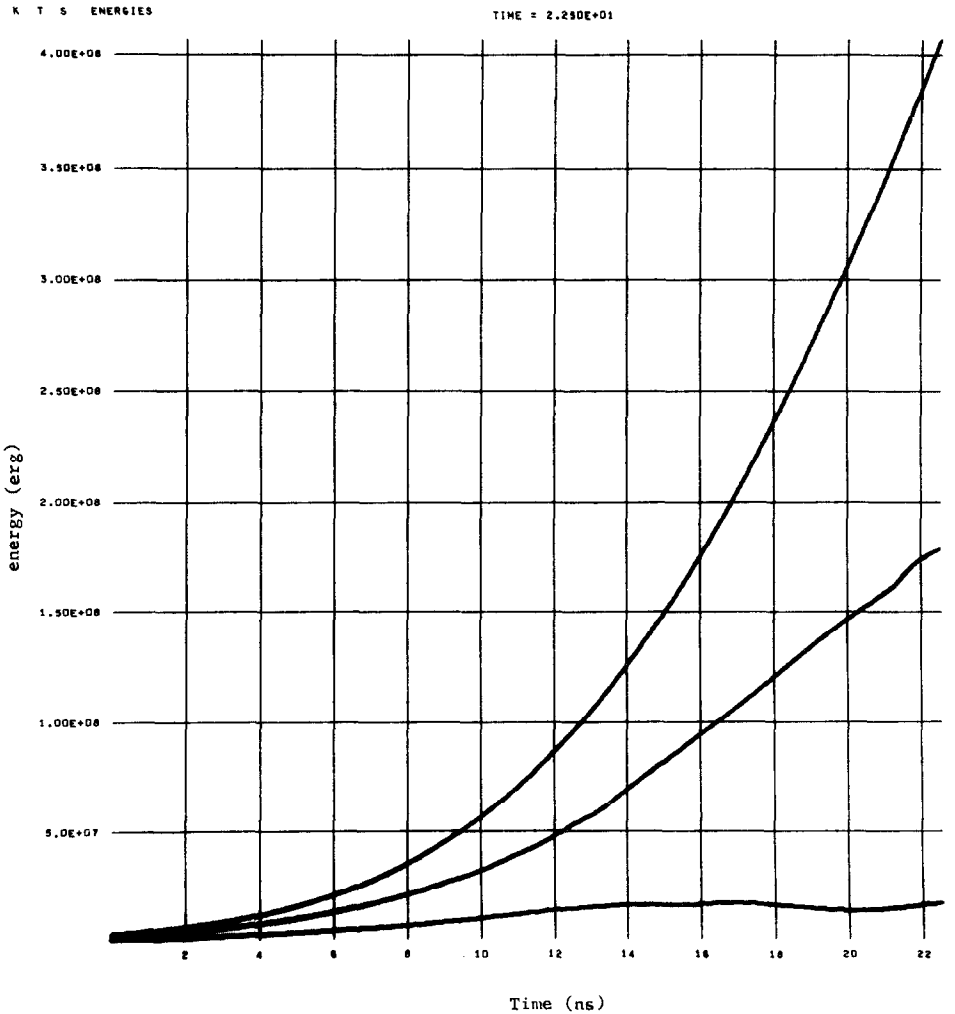

FIG. 10. Kinetic, thermal, and source energies in the plasma versus the time.

This method consists to keep more in line the velocity at a vertex (l, m) with the velocities of the other mesh at neighboring vertices with the relation:

$$\tilde{V}_{l,m} = (1 - \alpha)\, V_{l,m} + \frac{\alpha}{4}\,[V_{l+m,m-1} + V_{l+1,m+1} + V_{l-1,m+1} + V_{l-1,m-1}].$$

This has not been yet tried in this code. It is the opinion of the author that one should avoid the use of numerical schemes with independant meshes which are always troublesome.

One can use instead the two-step Lax–Wendroff scheme described by Lapidus [19] or apply a splitting technique [17].

ACKNOWLEDGMENTS

I am grateful for the stimulating discussions on the numerical aspects of this code by G. Basque. I also wish to thank D. Colombant for giving me the physic background and P. Figeac for allowing the publication of this research work which was supported by the French Atomic Energy Commission.

REFERENCES

1. I. BERNSTEIN AND W. FADER, Expansion of a resistive spherical plasma in a magnetic field, *Phys. Fluids* **11** (1968), 2209.
2. J. W. POUKEY, Expansion of a plasma shell into a vacuum magnetic field, *Phys. Fluids* **12** (1969), 1452.
3. A. HAUGHT, D. POLK, AND W. FADER, Magnetic field confinement of laser irradiated solid particle plasmas, *Phys. Fluids* **13** (1970), 2842.
4. T. P. WRIGHT, Early-time model of laser plasma expansion, *Phys. Fluids* **14** (1971), 1905.
5. R. GAJEWSKI, MHD equilibrium of an elliptical plasma cylinder, *Phys. Fluid* **15** (1972), 70.
6. I. LINDEMUTH AND J. KILLEEN, Alternating direction implicit techniques for two-dimensional magnetohydrodynamic calculations, *J. Computational Physics* **13** (1973), 181–208.
7. J. BAYARD, J. BOUJOT, M. MATTIOLI, AND J. SOULE, Rapport EUR-CEA FC 548, 1970.
8. J. BOUJOT, J. SOULE, AND R. TEMAN, Traitement numérique d'un problème MHD, *in* "Second international conference on numerical methods in fluid dynamics, Berkeley, September 1970."
9. D. COLOMBANT, M. RABEAU, D. SHIRMANN, AND G. TONON, Confinement of a laser created plasma by a 300 kG magnetic field, Gordon conference on laser interaction with matter, Beaver Dam, Wisconsin, August 1971.
10. J. FREEMAN AND F. LANE, Proc. A.P.S. topical conference on numerical simulation of plasma, LA 3990 (1968).
11. J. R. FREEMAN, Numerical studies of plasmoïd interaction with an axially symmetric magnetic field, *Nuclear Fusion* **11** (1971), 425.
12. Chocs et ondes de choc, tome 1, aspects fondamentaux, Masson et Cie, 1971.
13. A. JEFFREY, "Magnetohydrodynamics," Oliver and Boyd, 1966.

14. R. RICHTMYER AND K. MORTON, "Difference Methods for Initial-Value Problems," second ed., Interscience Publishers, New York, 1969.
15. "Methods in Computational Physics," Vol. 9, Academic Press, New York, 1970.
16. D. E. POTTER, Numerical studies of two-dimensional MHD initial value problem, with particular application to the plasma focus, Ph.D. Thesis, University of London, 1970.
17. N. N. YANENKO, Méthode à pas fractionnaires, collection intersciences, Armand Colin, 1968.
18. L. SPITZER, Physique des gaz complètement ionisés, monographies Dunod, Paris, 1959.
19. A. LAPIDUS, A detached shock calculation by second-order finite differences, *J. Computational Phys.* **2** (1967), 154.
20. C. W. HIRT AND A. A. AMSDEN, An arbitrary lagrangian-eulerian computing method for all flow speeds-LA-DC-72-1287, *J. Computational Phys.*, to appear.
21. F. FLOUX AND A. BILLEBIZE, Interaction laser—deuterium solide, étude numérique., Rapport CEA-R-4148, 1971.
22. D. SCHIRMAN, P. GRELOT, M. RABEAU, AND G. TONON, Étude interferométrique de l'expansion d'un plasma créé par laser., Rapport C.E.A.-R-4299, 1972.
23. D. COLOMBANT, NGUYEN TRONG THUC, AND J. RAGUIDEAU, Interaction d'un plasma produit par laser avec un champ magnétique intense., Rapport C.E.A. DO-035-W/PG, 1972.